KINEMATICS MODELING OF A HYBRID WHEELED-LEG PLANETARY ROVER

Javier Hidalgo and Florian Cordes

DFKI - Robotics Innovation Center
Robert-Hooke-Str. 5, 28359 Bremen, Germany

ABSTRACT

It is the goal of this manuscript to describe and analyze a complete kinematic model for hybrid wheeled-leg rovers and its applicability to Sherpa, a flexible rover with a complex actuation system. Differential kinematic equations of the hybrid legs are combined to form the composite equation for the rover motion. The model captures the 6 DoF pose (position and orientation) while traversing uneven terrains for hybrid systems and independently actuated joints. The kinematics model is analyzed in order to correctly propagate rover pose as input for a pose estimator in localization. Initial results from simulation are discussed for Sherpa navigation kinematics towards efficient pose estimation and dead reckoning.

Key words: robot motion, wheel odometry, rover kinematics, dead reckoning and planetary rovers.

1. INTRODUCTION

Up to now planetary rovers deployed on extraterrestrial surfaces made use of passive suspension systems (mostly the "Rocker-Bogie" suspension). Wheeled mobile robots are more energy efficient than legged robots on hard and smooth surfaces while active articulated robots with sophisticated mobility systems enable traversal over uneven terrain. Development of hybrid wheeled-leg solutions for the next generation of more capable systems with active suspension are currently ongoing. The ATHLETE [WLB$^+$07] family of rovers with completely active suspension or hybrid solutions with actively and passive suspension as in Scarab [BWW08] or Chariot[1] are only some of the developments currently in progress.

Rover kinematics plays fundamental roles in design, dynamic modeling, dead reckoning, control and wheel slip detection. As the control of an actuated suspension system is more complex, a motion model of the chassis is required to correctly command the desired trajectory and propagate the pose of the wheels as well as to reduce slip by proper maneuvering [TM05] [SSVO09]. Most efforts

---

[1] http://www.nasa.gov/mission_pages/
constellation/main/lunar_truck.html

on kinematics have concentrated either on planar two-dimensional space, i.e., translation in the x-y plane and heading [Vol, GFASH09] or in more sophisticated systems with passive articulate joints [TM05]. Typically, the kinematics modeling can be solved by two methods, the geometric or the transformation approach. The geometric approach is more intuitive but it is restrictive to the particular platform lacking of generalization [CW90]. The transformation approach is general and consistent by applying a series of transformations and Jacobian matrices to relate motion in the joint space to the Cartesian space, which main contribution is by Muir and Newman [MN86].

Extensive research with different reasoning is available in literature. Alexander *et al* [AM89] present a planar rigid body model considering a variable number of wheels. Campion *et al* [CBDN96] classified ordinary mobile robots into five types taking into consideration generic parts of the model equations. Other research into wheel-ground contact angle and pose estimation of robots moving on uneven surfaces can also be found [LS07].

As of today, the challenges and problems of hybrid structures have not been extensively described. The approach presented in this paper extends [TM05, MN86] in order to solve the complete kinematics of hybrid wheeled-leg rovers. The methodology is applied to the particu-

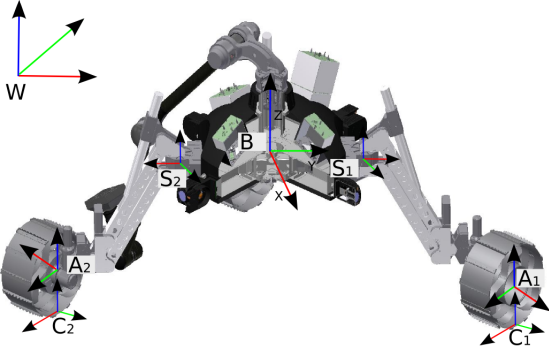Figure 1: The fully integrated Sherpa robot in a lunar testing environment.

Figure 2: Coordinate frames for the Sherpa rover. W is the world reference frame, B is the body frame, S_i is the swing leg-base frame, A_i is the wheel axle frame and C_i the wheel contact frame

Figure 3: General coordinate frames for wheel axle and contact point on inclined terrain. A_i is depicted here as x-axis pointing forward.

lar case of Sherpa which has a complex mobility system (see Figure 1). A six degrees-of-freedom (DoF) solution is pursued to propagate rover pose and velocity in a three dimensional space depending on the articulated joint configuration. The paper starts by describing a general kinematics model in Section 2. Afterwards, Section 3 analyzes its applicability to Sherpa. Different kinematics forms as the navigation kinematics (rover motion model) and the slip kinematics (wheel slip vector detection) are explained in Section 4. Uncertainty modeling and dead reckoning are presented in Section 5 to finally conclude with some results.

2. KINEMATIC MODELING

Wheeled-leg mobile robots consist of a number of legs connected to a main body and having a wheel at the end for rolling capabilities. Four main coordinate frames are defined, a robot body frame (B) attached to the rover center of mass, a swing leg-base frame (S) at the base of the leg, a wheel axle (A) frame attached to the wheel axle and a wheel contact frame (C) defined as a single point of contact between the wheel and the ground (see Figure 2). The B frame is related to a fixed navigation-frame (W) by the pose vector $\boldsymbol{U} = \boldsymbol{u}_{W,B} = (x\ y\ z\ \phi\ \theta\ \psi)$ Each wheel frame $A_i = 1, 2, 3, ..., m$ is related to the B frame by the transformation matrix $T_{B,A_i}(q)$ which depends on the particular leg kinematics in joints space represented by the vector $\boldsymbol{q} = [q_1\ q_2\ ...\ q_{n-1}]$ where n is the number of degrees of freedom of each leg.

The wheel is considered to be a rigid disc. A key difference between planar and articulated rovers for uneven terrain is the wheel contact angle δ_i at each C-frame defined as the angle between the normal vector to the terrain plane and the wheel z axis in A-frame (see Figure 3). Whereas the contact angle is always zero for planar mobile robots moving on flat terrains, it is a main distinction for articulated rovers and it is more important for hybrid wheeled-leg rovers which their suspension system allows actively control the angle.

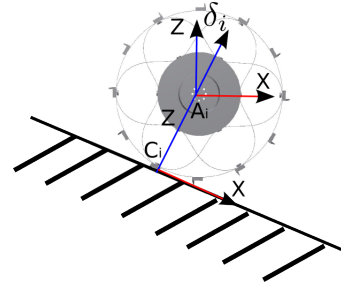The C-frame is related to the A-frame by the transforma-

tion matrix $T_{A_i,C_i}(\delta_i)$ defined as a rotation of the contact angle δ_i along the y axis and a translation in z-axis defined by the wheel radius r. The corresponding transformation matrix is given in (where c denotes cosine and s sine):

$$T_{A_i,C_i}(\delta_i) = \begin{bmatrix} c\delta_i & 0 & s\delta_i & -rs\delta_i \\ 0 & 1 & 0 & 0 \\ -s\delta_i & 0 & c\delta_i & -rc\delta_i \\ 0 & 0 & 0 & 1 \end{bmatrix} \quad (1)$$

The leg forward kinematics solution relating the wheel contact point with respect to the body is defined by the matrix multiplication $T_{B,C_i}(q,\delta_i) = T_{B,A_i}(q)T_{A_i,C_i}(\delta_i)$. Hybrid rovers also provide rolling capability which entails a change of the C_i frame over time increment Δt. The wheel motion is composite of a translation of the contact point along the x axis by $rq_{ni} + \xi_i$, where q_{ni} is the wheel rotation angle corresponding to the nth DoF of the leg i and ξ_i is the slip in the x direction. The slip vector can be modeled in three dimensions including lateral slip η_i along the y axis and rotational slip ζ_i along the z axis. The resulting transformation matrix is (where $\bar{C}_i$ is $C_i(k-1)$ and C_i is $C_i(k)$):

$$T_{\bar{C}_i,C_i} = \begin{bmatrix} c\zeta_i & -s\zeta_i & 0 & rq_{ni} + \xi_i \\ s\zeta_i & c\zeta_i & 0 & \eta_i \\ 0 & 0 & 1 & 0 \\ 0 & 0 & 0 & 1 \end{bmatrix} \quad (2)$$

The transformation of the body frame B with respect to the wheel contact point frame including the wheel rotation is:

$$T_{\bar{C}_i,B} = T_{\bar{C}_i,C_i}(q_{ni},\varepsilon_i)T_{C_i,A_i}(\delta_i)T_{A_i,B}(q) \quad (3)$$

where $\varepsilon_i = [\xi_i\ \eta_i\ \zeta_i]$ is the slip vector and the matrix $T_{C_i,A_i} = (T_{A_i,C_i})^{-1}$ and $T_{A_i,B} = (T_{B,A_i})^{-1}$

Mobile robots are commonly commanded by desired velocities. The mapping between the rover Cartesian space rate vector $\dot{\boldsymbol{u}} = \dot{\boldsymbol{u}}_{\bar{B},B} = \begin{bmatrix} \dot{x}\ \dot{y}\ \dot{z}\ \dot{\phi}\ \dot{\theta}\ \dot{\psi} \end{bmatrix}$ and the joint space rate vector $\dot{q}$, the wheel rotation rate $\dot{q}_{ni}$, wheel slip

rate vector $\dot\varepsilon_i$ and the wheel-ground contact angle rate $\dot\delta_i$ is solved by the Jacobian matrix. The velocity kinematics is deduced by applying the transformation matrix and the derivation of the point position relative to a coordinate system. Defining the transformation of the rover body at time step $k-1$ ($\bar{B}$) to rover body at time step k (B) as $T_{\bar{B},B} = T_{\bar{B},\bar{C}_i} T_{\bar{C}_i,C_i} T_{C_i,B}$, the derivative is

$$
\begin{aligned}
\dot{T}_{\bar{B},B} = {} & \dot{T}_{\bar{B},\bar{C}_i} T_{\bar{C}_i,C_i} T_{C_i,B} + \\
& T_{\bar{B},\bar{C}_i} \dot{T}_{\bar{C}_i,C_i} T_{C_i,B} + \\
& T_{\bar{B},\bar{C}_i} T_{\bar{C}_i,C_i} \dot{T}_{C_i,B}
\end{aligned} \tag{4}
$$

Considering that for a general body in motion the position and orientation rates of $\dot{T}_{\bar{B},B}$ are defined by the skew matrix:

$$
\dot{T}_{\bar{B},B} = \begin{bmatrix} 0 & -\dot\psi & \dot\theta & \dot x \\ \dot\psi & 0 & -\dot\phi & \dot y \\ -\dot\theta & \dot\phi & 0 & \dot z \\ 0 & 0 & 0 & 0 \end{bmatrix} \tag{5}
$$

Equating matrices in Equation 4 and 5 the velocity kinematics is obtained. The equation can be reordered in order to have the leg Jacobian matrix J_i of the form

$$
\begin{bmatrix} \dot x\ \dot y\ \dot z\ \dot\phi\ \dot\theta\ \dot\psi \end{bmatrix}^T = J_i \begin{bmatrix} \dot q\ \dot q_{ni}\ \dot\varepsilon_i\ \dot\delta_i \end{bmatrix}^T \tag{6}
$$

It defines the contribution of each leg to the body rover motion allowing the analysis of each joint to the resulting final velocity in $\dot{\boldsymbol{u}}$. The J_i matrix size is $6 \times (n+4)$ where n corresponds to the DoF of the leg. Finally, the composite rover equations are obtained combining the Jacobian matrices for all legs into a sparse matrix equation as

$$
\begin{bmatrix} I_6 \\ I_6 \\ \vdots \\ I_6 \end{bmatrix} \begin{bmatrix} \dot x \\ \dot y \\ \dot z \\ \dot\phi \\ \dot\theta \\ \dot\psi \end{bmatrix} = J \begin{bmatrix} \dot q \\ \dot q_n \\ \dot\varepsilon \\ \dot\delta \end{bmatrix} \equiv E\dot u = J\dot p \tag{7}
$$

where E is a $6m \times 6$ matrix that is obtained by stacking m 6×6 identity matrices, $\dot q$ is the $m(n-1) \times 1$ vector of rover joint angle rates, $\dot q_n$ is the $m \times 1$ vector of wheel rotation velocities, $\dot\varepsilon$ is the $3m \times 1$ slip vector and $\dot\delta$ is the $m \times 1$ vector of wheel-ground contact angle rates. The rover Jacobian matrix J is a $6m \times (mn + 4m)$ matrix obtained from the individual leg/wheel Jacobian matrices $J_i, i = 1, 2, ..., m$ and $\dot p$ is a $(mn + 4m) \times 1$ vector of composite angular rates for m leg/wheels of the rover.
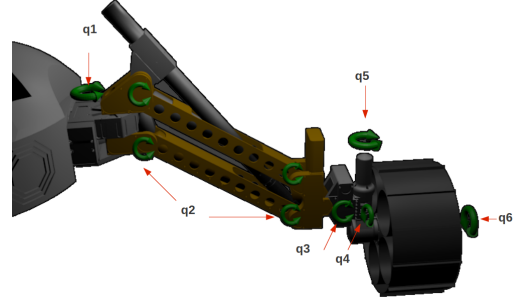

Figure 4: Detail of a Sherpa leg with the number of DoF

3. SHERPA ROVER

Sherpa [CDK11] is a hybrid wheeled-leg rover that is part of a multi-robot exploration system [CBLK10]. The rover is equipped with four legs with 4 DoF each, on these so called swing units are mounted the rover's wheels with 2 further DoF, one for steering the wheel and one for driving the wheel, respectively. More detailed information on Sherpa and the RIMRES project is provided in [CDK11, CRK12].

Sherpa is a highly capable planetary rover that is intended to serve as the central mobile unit in a multi-robot exploration scenario. It is able to manipulate payload-items that can be used to build up scientific or infrastructural components as well as for enhancing the capabilities of the mobile systems. The manipulator on top of Sherpa is used for handling the payload-items and for locomotion support [DRC11].

The wheeled-legs that constitute Sherpa's suspension system provide a total of 6 DoF each, summing up to 24 active DoF in the locomotion system. The first DoF (q_1) seen from the central body is called Thorax joint. The movement range is $\pm 90°$ around the vertical axis. The Basal joint (q_2) is designed as a parallel structure, that is responsible for lifting the wheel. These two DoF are the main DoF for (re-)positioning the wheel with respect to the body. The two auxiliary DoF WheelTilt (q_3) and WheelFlip (q_4) are used to orient the Wheel to the ground. By positioning a designated foot plate on top of the WheelSteering (q_5), the WheelFlip can be used to flip over the whole wheel and use a secure foot point[2]. WheelSteering (q_5) and WheelDrive (q_6) are used for steering and driving the wheel respectively. Figure 4 and Table 1 details the DoFs.

3.1. Sherpa Kinematic Model

Figure 5 illustrates the coordinate frames of a single leg of Sherpa according to Denavit-Hartenberg (D-H) notation. The D-H parameters $\theta, d. a$ and α are presented in Table 2 with units radians and millimeters. The presence of a parallel structure in the leg requires the definition of a virtual axes (Ba_2) which rotation angle (q_2)

---

[2]This feature is currently not implemented mechanically.

Table 1: Sherpas degrees of freedom of the suspension system and their specification

DOF	Name	Angle Limit (°)	Maximum Angular Velocity (°/s)	Repeatable Peak Torque/Force	Estimated std. deviation (°)
1	Thorax (Th)	± 90	12.0	$250\,Nm$	0.08
2	Basal (Ba)	± 60	13.3	$600\,N$	0.08
3	WheelTilt (WT)	± 30	6.7	$168\,Nm$	0.2
4	WheelFlip (WF)	± 180	23.4	$76\,Nm$	0.4
5	WheelSteering (WS)	± 90	75.0	$34\,Nm$	0.05
6	WheelDrive (WD)	cont. rot.	165.0	$50\,Nm$	0.02

is the negative value of the Basal joint (Ba). Wheel Tilt frame is rotated Φ radians along the z-axis in order to avoid the elbow between the virtual Basal joint and the Wheel Tilt. Wheel Flip frame appears to be outside of the mechanical structure between the steering and its predecessor frame in the chain (WT) with a displacement of $-HWF$ units along its x-axis. This choice of the coordinate frame ensures the minimum number of frames to represent the transformation between the wheel leg swing base (S) and the wheel contact point (C)

The resulting transformation from Sherpa body to the wheel contact point can be written as

$$T_{B,C_i(q,\delta_i)} = T_{B,S_i} T_{S_i,A_i}(q) T_{A_i,C_i}(\delta_i)\ \ i = 1,2,3,4 \tag{8}$$

The transformation from the body frame (B) to the leg

Table 2: D-H parameters for Sherpa Leg

Frame	θ	d	a	α
Th	q_1	0	LTh	$\Pi/2$
Ba	q_2	0	L	0
Ba_2	$-q_2 - \Phi$	0	D	0
WT	$q_3 + \Omega$	0	HWF	$\Pi/2$
WF	$q_4 + \Pi/2$	$LWT + LWF$	0	$\Pi/2$
WS	$q_5 + \Pi/2$	$-HWD$	LWD	0

$LTh = 90\,mm$ offset between the Th and the Ba frame
$L = 520\,mm$ forward distance between Ba and $Ba2$
$LBa = 88\,mm$ forward offset between $Ba2$ and WT
$LWT = 50\,mm$ horizontal offset between WT and WF
$LWF = 67\,mm$ horizontal distance between WF and WS
$LWD = 161\,mm$ offset between WS and A
$HWF = 29\,mm$ vertical displacement between WT and WF
$HWD = 100\,mm$ vertical offset between WS and A
$\Phi = \arctan\left(\frac{HWT}{LBa}\right)$ offset angle along the z-axis between Ba_2 and WF frame
$D = \sqrt{Lba^2 + HWT^2}$ displacement between the rotated $Ba2$ frame by Φ and the WF frame

swing base (S) (denoted in Equation 8 by T_{B,S_i}) is a fixed transformation depending on the leg position. Therefore, forward-right leg has a rotation of $45°$, forward-left of $-45°$, rear-left of $135°$ and rear-right of $-135°$ along the z-axis and a corresponding translation along x and y-axis. In order to be consistent to the right-handle frame notation and keep the x-axis in the C_i-frame pointing towards the forward motion of the wheel rotation, the transformation between A_i and C_i frames given by Equation 1 varies depending on the leg side. It results on a positive (right-side legs) or negative (left-side legs) $90°$ angle rotation along z-axis, which gives the following transformation matrices

$$T_{A_i,C_i}(\delta_i) = \begin{bmatrix} 0 & c\delta_i & s\delta_i & -rs\delta_i \\ -1 & 0 & 0 & 0 \\ 0 & -s\delta_i & c\delta_i & -rc\delta_i \\ 0 & 0 & 0 & 1 \end{bmatrix} i = 1,3 \tag{9}$$

$$T_{A_i,C_i}(\delta_i) = \begin{bmatrix} 0 & -c\delta_i & s\delta_i & -rs\delta_i \\ 1 & 0 & 0 & 0 \\ 0 & s\delta_i & c\delta_i & -rc\delta_i \\ 0 & 0 & 0 & 1 \end{bmatrix} i = 2,4 \tag{10}$$

It is noted that wheel-contact transformation depends on the articulated joints values q and the wheel-contact angle δ_i. The Jacobian matrices are calculated as explained in Section 2 using Equation 8. The computation of the velocity kinematics requires the derivative of transformation matrices, which for Sherpa rover there are a considerable amount of DoFs (10 DoF per leg coming from joints, wheel-ground contact angle and slip vector). The cascade velocity derivative corollary [MN86] is applied in order to simplify the derivation. Since T_{B,S_i} (and therefore $T_{S_i,B}$) is independent of time, the time derivative of $T_{\bar{B},B}$ is

$$\dot{T}_{\bar{B},B} = T_{\bar{B},\bar{S}_i} \dot{T}_{\bar{S}_i,\bar{C}_i} T_{\bar{C}_i,B} + \\ T_{\bar{B},\bar{C}_i} \dot{T}_{\bar{C}_i,C_i} T_{C_i,B} + \\ T_{\bar{B},C_i} \dot{T}_{C_i,S_i} T_{S_i,B} \tag{11}$$

where the first row represents the rate change of the wheel contact point at time $k-1$ with respect to the body frame.
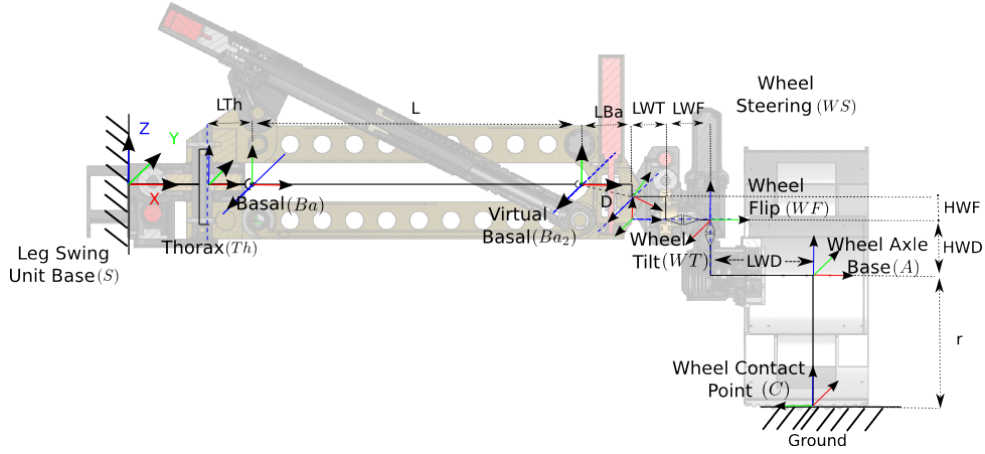
Figure 5: Coordinate frames for rover's leg at zero position. Note that the orientation of wheel contact point frame (C) depends on the leg side.

It involves leg lifting and is only applicable when walking mode is used by Sherpa (i.e, overcoming big obstacles), since walking machines do not provide continuous contact to the ground. The second row is the rate change of the wheel contact point due to wheel rotation. The third row is the Sherpa body frame rate change related to the ground contact point when adapting to the terrain.

This kinematic model defines different wheel Jacobian matrices depending on the locomotion mode. When the rover is walking over its wheels, no rotation is performed and only the slip vector rate defines the derivation of $\dot{T}_{\bar{C}_i,C_i}$. The derivative transformation $\dot{T}_{\bar{S}_i,\bar{C}_i}$ defines the first part of the walking cycle and $\dot{T}_{C_i,S_i}$ models the second part. In the majority of cases, when the robot is rolling over its wheels, the wheel contact point only changes due to wheel rotation and the first row of Equation 11 is set to zero while the third row defines the joints rate change due to actively terrain adaptation of the chassis.

The resulted $\dot{T}_{\bar{B},B}$ given by Equation 11 is equaled to the Equation 5 and the leg Jacobian of the form in Equation 6 is obtained for the Sherpa rover. Further, the composite rover equations are formed by combining the four legs Jacobian matrices in the form of Equation 7.

4. SHERPA KINEMATIC EQUATIONS

Different forms of rover kinematics can be obtained depending on the specific state of interest. This article focuses on two forms since the purpose is to properly model Sherpa rover kinematics towards an efficient pose estimation during path following. This will be done by describing useful forms of Equation 7 for Sherpa, referred as navigation kinematics and slip kinematics. Finally, uncertainty modeling and step-integration is performed to estimate rover pose over time using dead reckoning methods. Other forms of interest as leg-inverse kinematics and actuation kinematics to command desired rover velocities are also valuable to analyze [TM05], but they are beyond

the scope of this paper.

4.1. Navigation Kinematics

Navigation kinematics relates rover pose rate to the joints and sensed rate quantities. The navigation kinematics is often referred as motion model and is the basics for dead reckoning systems. The objective of the method is to estimate the rover pose. Moreover, it is useful for the understanding of the role of different quantities contributing to the final rover pose.

In order to simplify the model, the navigation kinematics focuses on the navigation form of Equation 11 when Sherpa is rolling over its wheels and adapting its legs to the uneven terrain. Therefore, the first row of Equation 11 is set to be zero since any walking movements are analyzed for the purpose of this work. Joint angle measurements are available in Sherpa rover since absolute encoders are installed in each joint and relative encoders are available in all wheels for measuring wheel rotation rates. Sherpa rover is also equipped with an IMU that can provide information on the pitch and roll angle, since they are able to compensate for drift error by estimation of the gravity vector using accelerometers. This is not totally possible by the heading error. Sensor availability defines sensed and not-sensed quantities and Equation 7 separates as

$$\begin{bmatrix} E_s & E_n \end{bmatrix} \begin{bmatrix} \dot{u}_s \\ \dot{u}_n \end{bmatrix} = \begin{bmatrix} J_s & J_n \end{bmatrix} \begin{bmatrix} \dot{p}_s \\ \dot{p}_n \end{bmatrix} \qquad (12)$$

Rearranging into not-sensed (right-side) and sensed (left-side) quantities, the resulting equation is obtained

$$\begin{bmatrix} E_n & -J_n \end{bmatrix} \begin{bmatrix} \dot{u}_n \\ \dot{p}_n \end{bmatrix} = \begin{bmatrix} -E_s & J_s \end{bmatrix} \begin{bmatrix} \dot{u}_s \\ \dot{p}_s \end{bmatrix} \equiv A\chi = B\gamma \qquad (13)$$

where A and B are matrices dimensions depends on the sensing capabilities of the rover system which will direct influence on the existence of a solution. The study the rank of A refers the sensing analysis of the navigation equations. There is no solution if the matrix A has not full-rank and therefore the system is undetermined. However, if $\text{rank}[A|B] = \text{rank}[A]$ the system is determined and a unique solution exits. When the system is overdetermined, $\text{rank}[A|B] > \text{rank}[A]$, there is more than one solution and least-square method is applied to solve the equations minimizing the error. If the matrix A has fully-rank and $\text{rank}[A|B] > \text{rank}[A]$, there is ample sensing because it provides extra sensing capabilities. This extra information is very useful for slip detection and error analysis where the equations are inconsistent [TM05].

All the joints angles and wheel rolling rates are sensed quantities, as well as the pitch $\dot{\phi}$ and roll $\dot{\theta}$ angles rates. The slip vector $\dot{\varepsilon}$ is not a sensed quantity and the wheel-ground contact angles $\dot{\delta}$ are defined here as unknown values even though some techniques can be used to estimate these angles [LS07] or by the installation of force sensors in wheel axles. Not-sensed quantities of the vector $\dot{u}$ are $\dot{x}$, $\dot{y}$, $\dot{z}$ and $\dot{\psi}$. Here, the slip vector $\dot{\varepsilon}$ is modeled as only rotation along its z-axis ζ_i since it is assumed no wheel slip with *nonholonomic* constraints. Then rows corresponding to x and y-axis elements of the slip vector can then be removed for the navigation kinematics. The resulting matrices E_n, E_s, J_n and J_s have dimensions 24×4, 24×2, 24×8 and 24×24 respectively. The matrix A and B have dimensions 24×12 and 24×26 respectively and χ is a 12×1 vector corresponding to the not-sensed quantities and γ is a 26×1 vector corresponding to the sensed quantities (i.e., rover joints, wheel rolling and pitch and roll angles). The solution for the Equation 13 is obtained using least-square method where the error vector is given as

$$e = B\gamma - A\chi \qquad (14)$$

the solution is based on minimizing the error vector $E = e^T C e$, where C is the constant matrix which could be the weighting matrix block diagonal, but for simplification here $C \equiv I$. The solution to Equation 13 is given by

$$\chi = (A^T C A)^{-1} A^T C B \gamma \qquad (15)$$

The desired quantities of Sherpa pose $\dot{x}$ $\dot{y}$ $\dot{z}$ are extracted by taking the first element of the solution vector χ. The least-square solution provide an optimal solution by minimizing the error e in velocity. This solution is applicable to dead reckoning methods. A large error represents larger navigation uncertainty, while a small error implies a more accurate solution.

4.2. Slip Kinematics

The detection of the slip vector ε is important to identify the terrain, correct odometry errors and reduce undesirable motions as well as detect the called 'slip-sinkage effect'. Similar to the navigation kinematics, the slip kinematics equation can be obtained per each rover leg/wheel. No-sensed values are worked out together at the right-side of the equation and sensed values are in the left-side

$$\begin{bmatrix} I_n & -J_{in} \end{bmatrix} \begin{bmatrix} \dot{\varepsilon}_i \\ \dot{\delta}_i \end{bmatrix} = \begin{bmatrix} -I_s & J_{is} \end{bmatrix} \begin{bmatrix} \dot{u} \\ \dot{q} \\ \dot{q}_{ni} \end{bmatrix}$$
$$A_i \chi_i = B_i \gamma_i , \ i = 1, 2, ..., m \qquad (16)$$

The analyses if the existence of a solution is similar to the navigation equations. The study the rank of A_i refers the sensing analysis of the slip equations. There is no solution if the matrix A_i has not full-rank and therefore the system is undetermined. The wheel slip rates could be fully detected if $\text{rank}[A_i|B_i\gamma] = \text{rank}[A_i]$ or equivalent to express the residual error equal to zero as

$$A_i(A_i^T A_i)^{-1} A_i^T - I B_i \gamma_i \ = \ P(A_i) - I B_i \gamma_i = 0 \quad (17)$$

where $P(A_i)$ is the projection matrix to the column space of the matrix A_i. When P is coincident with the identity the error is zero and a unique solution is found for the slip vector. For Sherpa rover, it is assumed that rover pose $\dot{u}$ is know using sensor capabilities as visual odometry or inertial sensors. The wheel contact angle is unknown and the joint rate angles and wheel rolling rate are known. With this configuration the resulting matrices I_s, J_{is} and J_{in} have dimensions 6×6, 6×6 and 6×4 respectively. The matrix A_i and B_i have dimensions 6×4 and 6×12 respectively, with not-sensed vector χ_i of dimension 4×1 and sensed vector γ_i of dimension 12×1.

5. EXPERIMENTS

Experiments with the real hardware are costly to perform and a proof-of-concept is needed as a first approach before testing with the real system. In order to evaluate the feasibility of the approach, a simulated terrain and the Sherpa rover in MARS (Machina Arte Robotum Simulans) [RKK09], a simulation and visualization tool for developing control algorithms and designing robots, is used. The simulator consists of a core framework containing all main simulation components, a GUI, OpenGL based visualization and a physics core that is currently based on ODE simulation environment. The simulation provides true position and orientation values, as well as information about wheel contact points with the ground. It is not the purpose of this work to accurately model surface conditions, the wheel-terrain interaction is based on

simple models. The output of the simulated rover is the sensed quantities as joint-angle vector $\boldsymbol{q}$, wheel rolling angles q_{n_i}, contact angles δ_i and ground truth for the pose vector $\boldsymbol{U}$.

5.1. Position Estimate Uncertainty and Results

Determining the uncertainty associated with robot's internal sensors is especially important since sensed values are usually corrupted by measurement errors. The uncertainty of the wheel-contact point is estimated with respect to the body frame. The information should be statistically relevant in order to be useful. A common assumption is to work with the first and second order centered moments of a calculated pdf ρ_ν, which is the expectation value $\bar{\nu}$ and the covariance matrix $\sum_{\nu\nu}$ (std. deviation is detailed in Table 1). Each DoF in the leg is modeled as a random value in the direction of the joint rotation which affects to the final pose uncertainty as a composition of transformations.

The angle uncertainty is then treated as a couple $(\bar{\nu}, \sum_{\nu\nu})$. A classical first order approximation of Jacobians described by Pennec *et al* in [PT97] is used to model the resulted noise of a chain of transformations along the leg. Therefore, rigid motions and the handling of uncertainty are done by composition of noise covariance matrix instead of additivity. The detailed derivation of the method is not reported here for brevity and can be found in [PT97].

The same noise propagation is used in the dead reckoning process. The least-squared solution of the navigation kinematics is the exact solution for the rover velocities under wheel no-slip assumption. The dead reckoning update calculation is described as

$$\boldsymbol{U}(k) = \boldsymbol{U}(k-1) + \frac{\Delta t}{2} R_{W,\bar{B}}(\dot{\boldsymbol{u}}(k-1) + \dot{\boldsymbol{u}}(k)) \quad (18)$$

where $R_{W,\bar{B}}$ is a rotation matrix from W-frame to $\bar{B}$-frame. It is assumed that the Sherpa motion is adequately modeled by constant accelerations since the robot is being actuated by constant force/torque generators in each sampling period Δt (the same sampling period as the dead reckoning process).The dead reckoning integration is erroneous when wheel slip occurs and visual techniques could be used to estimate the wheel slip vector described in Equation 17.

Two tests are presented here: a squared path and a serpentine path performed on inclined flat terrain by $15°$. Figure 6 depicts the pose estimator for the navigation kinematics and the dead reckoning method when the squared path is performed. An uncertainty of 0.12 m in x axis after 19 meters path is estimated considering internal errors coming from the encoders. Figure 7 show the pitch and roll angles propagation when initial pose is given and the angular rates $\dot{\phi}\ \dot{\theta}\ \dot{\psi}$ are not-sensed for a serpentine
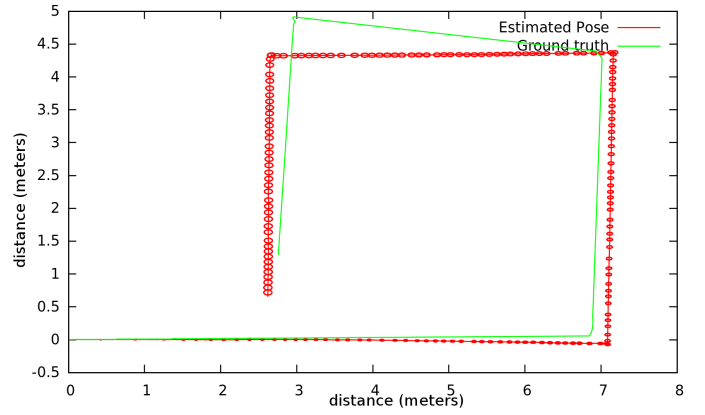

Figure 6: Pose estimation of Sherpa while performing a squared path on inclined terrain. The ellipse represent the rovers belief at different times.
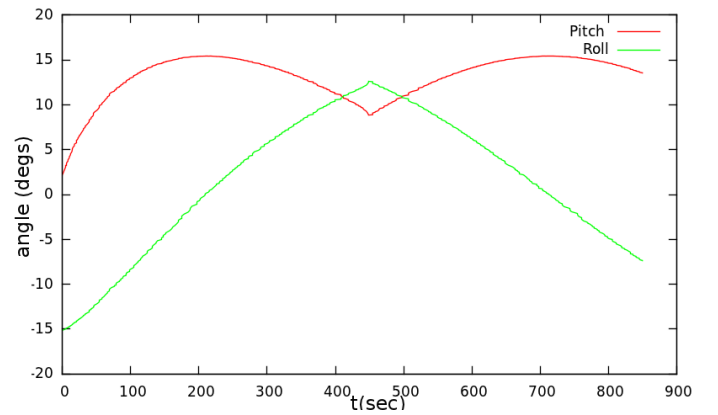

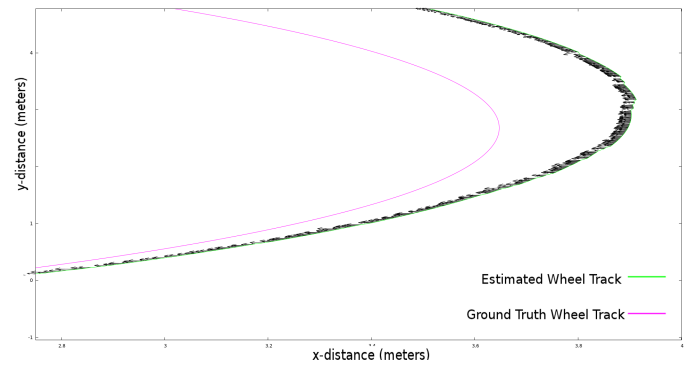Figure 7: Estimated pitch and roll angles when performing a serpentine path on inclined terrain.

Figure 8: Wheel track and slip vector estimation for the Front Right wheel on one of the turns of the serpentine path. Black arrows represent the direction of the estimated slip vector.

path. The navigation kinematics is used to estimate the change in attitude. Estimation of the wheel slip vector using Equation 17 is shown in Figure 8 demonstrating the applicability of the slip kinematics.

6. CONCLUSION

A methodology for the kinematic modeling and the pose estimation problem of a hybrid wheeled-leg robot is presented. Additionally, the wheel slip vector detection by the slip kinematics is also analyzed. The insight into kinematic modeling takes more importance for localization in space where methods can not make use of the Global Positioning System (GPS). Therefore, a six DoF solution in a three dimensional space is desirable for positioning during complex maneuvers and long term navigation by means of dead reckoning methods. The following objectives have been achieved. (1) Calculation of the leg/wheel forward kinematics and Jacobian matrices for the Sherpa rover. (2) Equations for the navigation and the slip kinematics for the Sherpa rover (3) Uncertainty modeling and propagation along the kinematic model due to measurement errors and (4) six DoF dead reckoning propagation. By using this method, all degrees of freedom are captured. Further analysis on the influence of each rover leg joint on the resulted robot pose is desired. Experiments with the real system should be performed to allow a more in-depth analysis in real environments.

REFERENCES

[AM89] J.C. Alexander and J.H. Maddocks. On the Kinematics of Wheeled Mobile Robots. *The International Journal of Robotics Research*, 8(5):15–27, October 1989.

[BWW08] Paul Bartlett, David Wettergreen, and William (Red) L. Whittaker. Design of the scarab rover for mobility and drilling in the lunar cold traps. In *International Symposium on Artificial Intelligence, Robotics and Automation in Space*, February 2008.

[CBDN96] Guy Campion, Georges Bastin, and Brigitte D'Andrea-Novel. Structural Properties and Classification of Kinematic and Dynamic Models of Wheeled Mobile Robots. *IEEE Transactions on Robotics*, 12:47–62, 1996.

[CBLK10] Florian Cordes, Daniel Bindel, Caroline Lange, and Frank Kirchner. Towards a modular reconfigurable heterogenous multi-robot exploration system. In *Proceedings of the 10th International Symposium on Artificial Intelligence, Robotics and Automation in Space (iSAIRAS'10)*, pages 38–45, August 2010.

[CDK11] Florian Cordes, Alexander Dettmann, and Frank Kirchner. Locomotion mode control for a hybrid wheeled-leg planetary rover. In *Proceedings of the IEEE International Conference on Robotics and Biomemetics (IEEE-Robio 2011)*, Phuket, Thailand, September 2011.

[CRK12] Florian Cordes, Thomas M. Roehr, and Frank Kirchner. Rimres: A modular reconfigurable heterogeneous multi-robot exploration system. In *Proceedings of the 11th International Symposium on Artificial Intelligence, Robotics and Automation in Space (iSAIRAS'12)*, 2012.

[CW90] Ingemar J. Cox and Gordon T. Wilfong, editors. *Autonomous robot vehicles*. Springer-Verlag New York, Inc., New York, NY, USA, 1990.

[DRC11] Alexander Dettmann, Malte Roemmermann, and Florian Cordes. Evolutionary development of an optimal manipulator arm configuration for manipulation and rover locomotion. In *Proceedings of the IEEE International Conference on Robotics and Biomemetics (IEEE-Robio 2011)*, September 2011.

[GFASH09] P. Robuffo Giordano, M. Fuchs, A. Albu-Schaffer, and G. Hirzinger. On the kinematic modeling and control of a mobile platform equipped with steering wheels and movable legs. In *IEEE International Conference on Robotics and Automation*, pages 4080–4087. Ieee, May 2009.

[LS07] P. Lamon and R. Siegwart. 3D Position Tracking in Challenging Terrain. *The International Journal of Robotics Research*, 26(2):167–186, February 2007.

[MN86] Patrick F Muir and Charles P Neuman. *Kinematic Modeling of Wheeled Mobile Robots*. Number June. 1986.

[PT97] Xavier Pennec and Jean Philippe Thirion. A Framework for Uncertainty and Validation of 3-D Registration Methods Based on Points and Frames. *International Journal of Computer Vision*, 25:203–229, 1997.

[RKK09] Malte Rommerman, Daniel Kuhn, and Frank Kirchner. Robot design for space missions using evolutionary computation. In *2009 IEEE Congress on Evolutionary Computation*, pages 2098–2105. Ieee, May 2009.

[SSVO09] Bruno Siciliano, Lorenzo Sciavicco, Luigi Villani, and Guiseppe Oriolo. *Robotics. Modeling, Control and Planning*. 2009.

[TM05] Mahmoud Tarokh and Gregory J Mcdermott. Kinematics Modeling and Analyses of Articulated Rovers. *IEEE Transactions on Robotics*, 21(4):539–553, 2005.

[Vol] R. Volpe. Inverse Kinematics for All-Wheel Steered Rovers. Technical report.

[WLB+07] B.H. Wilcox, T. Litwin, J. Biesiadecki, J. Matthews, M. Heverly, J. Morrison, J. Townsend, N. Ahmad, A. Sirota, and B. Cooper. Athlete: A cargo handling and manipulation robot for the moon. *Journal of Field Robotics*, 24(5):421, 2007.